Thermal and mechanical properties of polyethylene glycol (PEG)-modified lignin/polylactic acid (PLA) biocomposites

Zehui Ju, Nicolas Brosse, Sandrine Hoppe, Zhiqiang Wang, Isabelle Ziegler-Devin, Haiyang Zhang, Biqing Shu

Thermal and mechanical properties of PEG-modified lignin / polylactic acid biocomposites

Zehui Ju[a,b,c*], Nicolas Brosse[c*], Sandrine Hoppe[d], Zhiqiang Wang[a,b], Isabelle Ziegler-Devin[c], Haiyang Zhang[a], Biqing Shu[e]

[a] College of Materials Science and Engineering, Nanjing Forestry University, Nanjing, 210037, PR China

[b] Co-Innovation Center of Efficient Processing and Utilization of Forest Resources, College of Materials Science and Engineering, Nanjing Forestry University, Nanjing 210037, China

[c] Université de Lorraine - INRAE - LERMAB - GP4W, F 54000 Nancy - France

[d] Université de Lorraine - CNRS - LRGP, F 54000 Nancy, France

[e] College of Civil Engineering, Yangzhou Polytechnic Institute, Yangzhou, 225127, P.R. China

Abstract:

In this study, a method was proposed to prepare biocomposites from polylactic acid and polyethylene glycol (PEG) modified lignin using twin-screw extrusion process. The structure of PEG modified lignin was studied by Fourier Transform Infrared Spectroscopy (FTIR) and Gel permeation chromatographic (GPC) analysis. The effects of different contents of soda lignin and PEG modified lignin on PLA

composites were studied by tensile test, differential scanning calorimetry (DSC), thermogravimetric analysis (TGA), scanning electron microscopy (SEM), dynamic mechanical analysis (DMA) and degradation analysis. The experimental results showed that the addition of PEG modified lignin improved the heat resistance of PLA composite. PLA could be combined with up to 30% PEG-modified lignin, with no significant reduction in tensile strength properties. Compared with PLA-L30, the tensile stress and elongation at break of PLA-PL30 were increased by 26.4% and 78.9%, respectively. This approach provides a new way to produce high-performance lignin based-PLA composites.

Keywords: PLA, PEG-modified lignin, biocomposites, thermal and mechanical properties, degradation

1. Introduction

3D printing belongs to rapid prototyping technology and additive manufacturing technology that enable materials to be manufactured by stacking them layer by layer. This technology is one of the core technologies of the third industrial revolution **[1]**. The development of 3D printing technology is very rapid, the technology has been widely used in different industries, such as industrial manufacturing, construction, national defense and aerospace, education and training, biomedical and other fields **[2]**. The technology has obvious digital characteristics. In the current 3D printing technology market, fused deposition molding (FDM) is the most widely used printing technology at present. The FDM equipment is mainly composed of wire feeding

device, heating device, motion mechanism, control panel, printing device and workbench **[3]**. The mainstream materials commonly used in today's market for FDM printing are the following: Acrylonitrile Butadiene Styrene (ABS) plastics, polycarbonate, polyamide, polylactic acid (PLA) **[3]**.

Traditional petroleum-based polymers are non-renewable resources. The intensive use of these polymers has harm effects on the environment. The development and research related to these non-renewable materials is starting to gradually decline in favour of more sustainable polymers **[4]**. Polylactic acid (PLA) is one of the most commercially developed renewable and biodegradable polymer **[5]**. PLA can be synthesized by direct condensation polymerization of lactic acid monomer or ring-opening polymerization of cyclic lactide monomer, both of which can be obtained by fermentation of corn starch, sugarcane or other renewable biomass **[6-8]**. In addition to the biological properties of the material itself, PLA also has outstanding mechanical and physical properties, such as high modulus, high strength, ease of processing, transparency and so on. The tensile strength of PLA can reach 50 - 70 MPa, elastic modulus up to 3 - 4 GPa **[9]**. However, the rigidity of the main chain structure of PLA material determines the weak impact strength and low fracture elongation of PLA, which limits its use in a wide range of fields **[8, 10]**. Another major shortcoming of PLA is its low crystallization rate, which results in low PLA crystallinity and a low heat distortion temperature, limiting its field of application. Given the advantages and disadvantages of PLA, as well as the diversification and complexity of its use, significant research is being carried out to improve its overall

performance through the production of low-cost PLA-biobased composites. **[7, 11]**, **[12]**.

Lignin, a renewable macromolecule **[13]** and an abundant co-product of the pulp industry, is of particular interest as a possible filler for PLA-based composites. It is estimated that the paper industry can produce about 70 million tons of lignin per year, which is mainly used for energy production. Il is estimated that only 2% of the lignin is processed for non-energy application. Lignin, the only non-petroleum resource capable of providing renewable aromatic compounds, has been the focus of particular attention by many researchers, who have sought to develop its rational and valuable use. **[16]**. The molecular structure of lignin is composed of many aryl ring structures connected by ether bonds and carbon-carbon bonds, which gives lignin high rigidity and high thermal stability **[14]**. At the same time, its phenol-rich structure gives interesting properties such as antioxidant, ultraviolet adsorbent, antibacterial agent and so on **[19, 20 [17]**. As a result, the design of composites based on lignin and polymer materials not only adds value to lignin, but can also lead to the design of high-performance polymer materials including 3D printed materials **[20]**. However, researchers **[11, 21-22]** found that lignin can enhance the mechanical properties of PLA to a certain extent, but the compatibility between lignin and PLA is poor, and the strength of the composite cannot be further improved. At the same time, The performance of lignin /PLA prepared by blending is poor, which affects the feasibility of commercialization, mainly because of the thermal degradation of lignin during processing, and the uneven agglomeration and dispersion caused by its strong polarity,

resulting in the decline of interface binding force **[23]**. So chemical modifications are required to improve the composite interface. The Nam team modified lignin by acetylation to enhance the compatibility of Lignin and PLA and prepared the bio-based PLA / lignin composite membraneby solvent volatilization **[24]**. Wasti et al. **[22]** studied adding the plasticizer PEG to PLA/Lignin composite to improve the mechanical properties of the composite. Steam explosion pretreatment of biomass was used for the application of PEG plasticized lignin, and the results showed that the thermal properties of the prepared PEG modified lignin were improved. There are few studies (referneces) on the application of PEG modified lignin as biological filler in PLA, the compatibility of PEG modified lignin with PLA, and the thermal, mechanical and morphological properties of biocomposites.

In this study, we will focus on developing a new method of PEG-modified lignin as filler in 3D printing material polylactic acid and explore the feasibility of FDM 3D printing. Alkaline lignin and PEG modified lignin were prepared by steam blasting pretreatment of beech wood under two processes of alkali delignification and acid catalyzed polyethylene glycol (PEG) delignification. The properties of lignin were characterized by high performance liquid chromatography (HPLC), Fourier transform infrared spectroscopy (FTIR) and Gel permeation chromatographic (GPC). The lignin / PLA composite was prepared by twin-screw extruder mechanism. The mechanical properties, morphology, thermal properties and water absorption of the composite were studied. The effects of lignin on the properties of PLA were examined by Differential Scanning Calorimetry (DSC), Thermogravimetric analysis (TGA),

Dynamic mechanical analysis (DMA), mechanical properties and so on. The microstructure of the composite was analyzed by SEM. At the same time, the degradation rate of biocomposite in the aquatic system was studied. Based on this, the application of PLA materials in various fields was expanded, and the goal of replacing traditional petroleum-based polymer materials was realized. The central hypothesis of this study was that PEG modified lignin can improve the compatibility of lignin / PLA and thus improve the mechanical properties.

2. Materials and Experiments

2.1 Materials

In this study, beech (*Fagus longipetiolata*, Lorraine, Vosges France) was crushed to 3 - 8 cm. The beech sawdusts were dried to a moisture content of 8.3% in a natural state as raw material for lignin preparation. Polyethylene glycol 600 (PEG 600), the sodium hydroxide and the sulfuric acid were purchased from Merck KGaA, Darmstadt, Germany. PLA (Grade 4032D, Mw = 94,000 g/mol) was provided by Nature works LLC (Minnesota, USA). Three buffers (phosphate buffer (pH = 4.0), sodium carbonate buffer (pH = 10.0), and phosphate Buffered Saline (PBS, pH = 7.4)) obtained from Xiamen Sea Standard Technology Co., LTD were used for degradation tests.

2.2 Preparation of PEG-modified lignin/PLA biocomposites

2.2.1 Steam-explosion (SE) pretreatment

Beech sawdusts (200g) were impregnated in 1% sulfuric acid solution for 15 hours. After soaking, the solids were removed and dried at 50 °C for 24 h. Then the impregnated beech wood were putted into the steam explosion device, and the steam explosion experiment parameter was 210 °C for 2.5 min. After treatment, the biomass were collected from steam explosion device, and the filtered solid residue was washed with distilled water to remove the degradation substances, and dried at 70 °C for 48 h.

2.2.2 Soda lignin preparation

The steam explosion treated biomass was placed in a 500 mL flask, 1% NaOH solution was added in flask. The flask was putted ia thermostat water bath at 80 °C for 2 h. After extraction, the filtered solid residue was washed to neutral, dried at 70 °C for 48 h. The pH value of the filtrate was adjusted to 5.0 - 5.5 by 5 mol/L H_2SO_4 solution, and then the mixture was thoroughly dialysis with distilled water (dialysis in a 5 L container for 1 week; Change the distilled water twice a day). After centrifugation (12100 rpm, 10 min), the soda lignin was dried at 40 °C for 48 h.

2.2.3 Polyethylene glycol (PEG)-modified lignin preparation

PEG-600 containing 0.3% sulfuric acid was reacted with the steam explosion treated biomass at 140 °C for 90 min, and the solid-liquid ratio was 5/1. After the reaction, 0.2 mol/L NaOH solution was added in the mixture as diluent and stirred evenly. Then the solid residue after vacuum filtration was washed and filtered with distilled water. The liquid phase was evenly mixed with the washed water. The pH of

the filtrate was adjusted to 5.0-5.5 with 5 mol/L H_2SO_4 solution, and then the mixture was thoroughly dialysis with distilled water (dialysis in a 5 L container for 1 week; Change the distilled water twice a day). After centrifugation (12100 rpm, 10 min), the PEG-modified lignin was dried at 40 °C for 48 h.

2.2.4 Composite filament preparation

Polylactic acid (PLA) was ground into powder by a grinder to ensure adequate mixing with the lignin. PLA and lignin were dried at 80 °C for 6 hours, respectively. The composition of the filaments was according to the **Table 1**. Twin-screw extruder (Thermo Science ™ Process 11, Villebon-Sur-Yvette, France) was used to mix PLA powder and lignin, and the two mixing zones of the screw profile can guarantee a high level of uniform dispersion of lignin in PLA. The twin-screw extruder had 8 temperature zones, the setting range was 1- 8: 154 ◦C, 160 °C, 170 °C, 175 °C, 178 °C, 180 °C, 180 °C, 180 °C, 180 °C. The screw nozzle diameter was 4 mm. The speed was set at 50 rpm. By controlling the rotation of the spool and the speed of the conveyor belt, a filament with a diameter of 1.75 ± 0.1 mm that can be used for 3D printing was obtained, and these filaments were dried at 50 °C for 24 h to remove free water from the surface.

Table 1 The composition of the filaments

Sample notations	PLA (wt%)	Soda lignin (wt%)	PEG modified lignin (wt%)
PLA	100		

PLA-L10	90	10	
PLA-L20	80	20	
PLA-L30	70	30	
PLA-PL10	90		10
PLA-PL20	80		20
PLA-PL30	70		30

Note: PLA- Polylactic acid, L-Soda lignin, PL- PEG modified lignin.

2.2.5 D printing process

The FDM printer used in the experiment was MakerBot Replicator 2 (MakerBot Inc., USA), and the software for regulating and monitoring in the 3D printing process was Repetier Host 1.0.6. A 3D dynamic mechanical analysis (DMA) model with the dimensions of 40 mm×10 mm×2 mm was prepared, and a dog bone sample according to ASTM D638 type V was obtained. The filaments used for 3D printing were prepared by the twin-screw extrusion mechanism, the diameter of the filaments were controlled at about 1.75mm, the temperature of the nozzle during printing was 210 °C, the temperature of the working platform was 60 °C, the filling Angle was set to 45°, the filling type was selected as 100% solid filling, the filling interval was selected as 0%, and the sample printing speed was 30 mm/s.

2.3 Lignin characterization

2.3.1 FTIR

The chemical structure of lignin was analyzed by Fourier transform infrared spectrometer (Thermo Electron Nicolet 380, Thermo Scientific, United States). First, the dried lignin and potassium bromide powder were fully ground in a mortar and pressed into tablets. Then the prepared potassium bromide tablets were placed into the instrument and scanned 32 times at room temperature in the range of 4000 - 400 cm^{-1}. The resolution was 4 cm^{-1}, and the data collection was completed.

2.3.2 Lignin composition

Lignin composition was analyzed according to the analytical methods of the National Renewable Energy Laboratory (NREL). 0.1 g sample was treated with 4mL (72% H_2SO_4) at 40 °C for 60 min. Then, the mixture was diluted to 4% and autoclaved at 121 °C for 67min. Glucose, pentose, and ethanol were tested by HPLC (UltiMate 3000, Thermofisher, USA) with UV and parallax detectors. The mobile phase was 5 mmol / L H_2SO_4. The flow rate was 0.6 mL/min.

2.3.3 Gel permeation chromatographic (GPC) analysis

The molecular weight of lignin **[25]** was determined by gel permeation chromatography (GPC, Agilent1200, USA). A certain amount of the sample was accurately weighed and dissolved in tetrahydrofuran (THF) to obtain 2 mg / mL solution. The solution was filtered by an organic filter with a pore size of 0.22 μm, and then proceeded to the chromatographic column (PLgel Mixed-D, 7.5 × 300 mm, Agilent, USA). The mobile phase was pure THF, and the flow rate was l mL / min.

The injection volume was 10 μL. The standard curves were calibrated with four polystyrene standard samples of different molecular weight (molecular weight: 66000, 9200, 1320 and 580 g/mol, respectively).

2.4 DSC

The crystallization and melting behavior of the samples were measured by differential scanning calorimetry (DSC, 204 F1,Germany Nechi instrument manufacturing Co., LTD). The sample was taken about 4g, and putted into the aluminum crucible. The samples were heated from room temperature to 200 ℃ at a rate of 10 °C / min. After the heating stops, the temperature was stopped for 5min to eliminate the thermal effect, and then the temperature was cooled to room temperature at 10 °C / min. After the cooling was completed, the temperature was kept for 5min. At last, the temperature was raised from room temperature to 200℃ at 10℃/min. The crystallization behavior and melting behavior of the samples under different conditions were studied by analyzing the DSC curves during cooling and second heating. The crystallization percentage (X_c, %) was estimated using the following equation:

$$X_c(\%) = \frac{H_m - H_{cc}}{H_m^0 \times w} \times 100\ \% \quad (1)$$

Note: X_c was crystallinity. *Hcc* was enthalpies of crystallization. *Hm* was enthalpies of Melting. H_m^0 was the enthalpy of PLA when completely melted, its value was 93.7 J/g. *w* was the weight fraction of PLA.

2.5 TGA

The thermal stability of the material was carried by a TG209 thermogravimetric analyzer (Netzsch, Germany). The test weight of the sample was 8 mg. The test environment was nitrogen atmosphere and the protection gas was also nitrogen. The flow rates were 20 mL / min, the heating rate was 10 °C / min, and the test temperature ranged from room temperature to 800°C. The thermogravimetric curve was obtained by scanning.□ □

2.6 DMA

DMA was performed in single cantilever mode using a dynamic thermo-mechanical analyzer (SDTQ800, V21.3, Build 96, USA). The test temperature was raised from room temperature to 100 °C, the heating rate was 5 °C / min, the frequency was 1 Hz, and the strain was 0.3%. The dynamic mechanical properties were tested in an air atmosphere, and the storage modulus (*E'*), loss modulus (*E''*) and loss factor (*tanδ*) of the sample were measured and recorded. All mechanical properties data were based on the average results of 5 different tests.

2.7 Mechanical testing

The dog bone samples were tested by EN ISO 527:1996 on instron tensile testing machine (Model 5569, Norwood, MA, USA). The tensile test rate was 1 mm / min, the bending rate was 1 mm / min, and the maximum bending tolerance was 6mm. The tests were carried out at room temperature. 5 samples were taken from each group for

testing, and the average value was obtained.

2.8 Scanning Electron Microscopy (SEM)

Scanning electron microscopy (SEM, Quanta 200, FEI, Netherlands) was used to observe the fracture surface morphology, the distribution of each phase component and the interface bonding of the composite. Before the test, in order to make the sample better conductive imaging, it was necessary to spray gold twice under vacuum conditions.

2.9 Water absorption

The water absorption of composite materials was carried out in accordance with the Chinese standard GB/T1034-2008 "Experimental method for Water absorption of plastics". First, the composite materials were dried in an oven at 80 °C for 6 h to remove free water, and then its weight (W_0) was weighed with an analytical balance. After weighing, the sample was putted into a 500mL beaker and an appropriate amount of distilled water was poured into it to make sure that the sample can be completely immersed in water for 50 days. After 50 days, the composite materials were dried in vacuum drying at 80 °C for 6 hours. Then the weight was recorded as W_1. Five samples were measured in each group, and the test results of the five samples were averaged to ensure the accuracy of the experiment. The water absorption of PLA biocomposites were calculated according to the following equation:

$$Water\ \ absorption\ \ (\%) = \frac{|W_1 - W_0|}{W_0} \times 100 \quad (2)$$

2.10 Immersion in solvent

The PLA / lignin composite was cut into 2.5 × 30 × 2 mm sample, and placed in buffer solution (pH = 4, pH = 10) and PBS solution (pH 7.4) at room temperature for hydrolysis performance test. The initial weight (W_0) of each sample was recorded before testing. After 50 days in solution, the sample was washed by distilled water, dried in an oven at 40 °C for 24 h, and the weight of each sample was recorded as W_1. The weight loss was calculated according to *formula (2)*.

3. Results and Discussion

A figure describing the method of production of lignin could help ! + one or 2 sentences here to explain the process in short

3.1 Lignin characterization

3.1.1 FTIR

Two kinds of lignin were preliminarily analyzed by FTIR. The result was shown in **Fig. 1**. The FTIR band fractions of lignin was shown in **Table 2 [26]**. In **Fig.1a**, the characteristic peak of -OH in the lignin extracted by PEG delignification shifted toward a lower wave number (3345 cm^{-1}) compared with soda lignin (3423 cm^{-1}). The results showed that the molecular structure of PEG and lignin formed a large degree of intramolecular hydrogen bond. The absorption peak strength at 2873 cm^{-1} was higher than that of soda lignin, due to methylene and methyl groups in PEG-modified

lignin **[27]**. As can be seen from **Fig. 1b**, new peaks appeared at 1352 cm^{-1} and 1250 cm^{-1}, which belonged to C-H shear vibration and C-O shear vibration of PEG respectively. In addition, compared with soda lignin, the ether groups of PEG-modified at 1121 cm^{-1} lignin were widened and moved toward lower wave number. New peaks were appeared at 1111 cm^{-1} and 949 cm^{-1}. In fact, 1111 cm^{-1} and 949 cm^{-1} assigned to the vibrations of C-O-C and C-OH in PEG **[28]**, respectively. It should be noted that the characteristic signals of the PEG group remain present even after intensive washing of the PEG-lignin, suggesting a covalent graft.

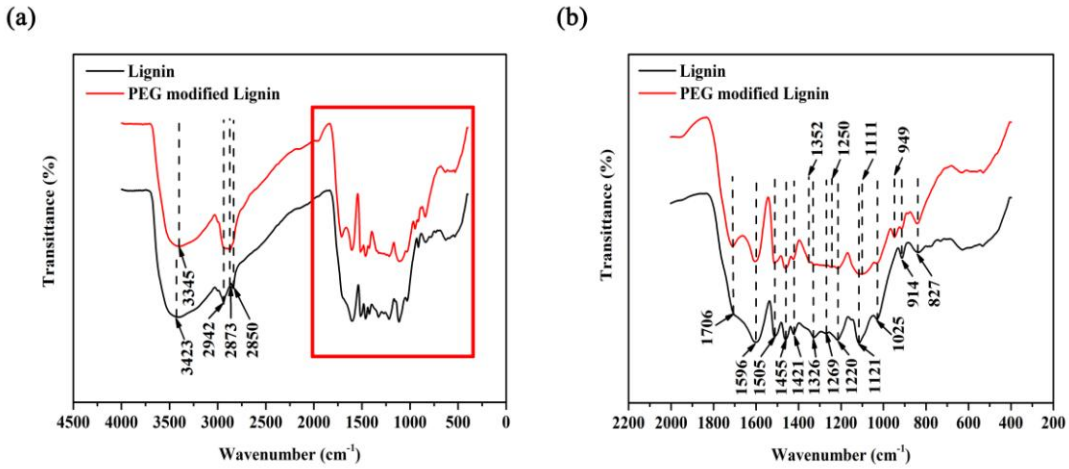

Figure 1 FTIR spectra for different lignin samples (a) lignins within 4000-400 cm^{-1}, (b) lignins within 2000-400 cm^{-1}

Table 2 Position and assignment of IR bands measured by FTIR

Band (cm^{-1})	Vibration	Assignment
3423	O−H stretching vibration	phenolic OH + aliphatic OH
3417		phenolic OH + aliphatic OH +

		PEG OH
3345		phenolic OH + aliphatic OH + PEG OH
2942	C−H stretching vibration	CH_3 + CH_2
2873	C−H symmetric stretching in methyl	CH_3 + CH_2
2850	C−H stretching in methylene group	OCH_3
1706	C=O stretching in unconjugated ketone	C = O
1596	aromatic skeletal vibrations plus C=O stretching	C = O
1505	C−C stretching vibration	aromatic skeleton
1455	C−H deformations	CH_3 + CH_2
1421	C−C stretching vibration	aromatic skeleton combined with C-H in plane deformations
1352	C–H shear vibration	PEG CH_3 + CH_2
1326	C− O stretching vibration	S
1269	C− O stretching vibration	G
1250	C− O stretching vibration	PEG
1220	C− O (H) stretching vibration	phenolic OH
1121	C−H in-plane deformation vibration	G
1111	C− O − C, stretching vibration	PEG
1025	Aromatic C-H in plane deformation	G + S
949	C–OH, asymmetric scissoring vibration	PEG OH
914	Ar C−H, out-of-plane	G

	deformation vibration	
827	C−H, out of plane in positions 2, 5 and 6	G + S

3.1.2 Lignin composition

Table 2 showed the yield and composition of the two kinds of lignin. In both cases, acid insoluble lignin (AIL) was greater than 90%, indicating that the lignin prepared in this study had high purity. After acid-catalyzed PEG delignification, the purity of lignin was improved to a certain extent. In addition, according to previous study **[29]**, some residual carbohydrates that may come from the lignin-carbohydrate complex have been detected. The contents of glucose and xylose after alkali delignification were higher, indicating that this method promoted the degradation of polysaccharides in a larger extent.

Table 3 Lignin yield and carbohydrate compositions of the lignin fraction

Sample	Yield	Compositions (%)								
	(%)	AIL	Glc	Xyl	Ara	Gal	Rha	GalUA	GlcUA	Total
Soda	14.39	94.14	0.74	0.05				0.23 ±	0.21 ±	1.04
lignin	±	±	±	±				0.01	0.01	±

	1.21	1.75	0.09	0.01			0.07
PEG	13.57	99.03	0.39				0.85
modified	±	±	±		0.20 ± 0.01	0.13 ± 0.01	±
lignin	1.01	1.18	0.01				0.01

3.1.3 GPC analysis

The weight-average molecular weight (Mw) and number-average molecular weight (Mn) of lignin were measured by GPC. The Mw, Mn and Mw/Mn of milled wood lignin was Mw=1926 and Mn=1265, Mw/Mn=1.52. It can be seen from **Table 4** that the Mw, Mn and Mw/Mn of both soda lignin and PEG modified lignin was decreased, mainly because steam explosion promotes the hydrolytic breakdown of lignin β-O-4 inter-units and reduced its molecular weight **[28, 30]**. It was also found that the Mw and Mn of PEG modified lignin were higher compared to soda lignin, confirming the pegylation reaction between PEG and lignin **[30]**. In addition, the dispersion index (Mw/Mn) of PEG modified lignin increased, indicating that PEG delignification not only degraded the lignin macromolecules to a some extent, but also led to an increase of molecular weight heterogeneity.

Table 4 Weight-Average Molecular Weight, Number-Average Molecular Weight, and Mw/Mn of Lignins

Sample	M_w	M_n	M_w/M_n
Soda lignin	701 ± 11	433 ± 7	1.62 ± 0.04

PEG modified lignin	1231 ± 12	672 ± 8	1.83 ± 0.03

3.2 DSC

Fig. 2 gave the differential scanning calorimetry (DSC) of Lignin/PLA composites, and **Table 5** was the transition temperatures and enthalpies of PLA and PLA/lignin composites. As shown in **Fig. 2** and **Table 5**, the glass transition temperature (Tg) of pure PLA was 59.3 °C. The soda lignin/ PLA composites (PLA-L10, PLA-L20, PLA-L30) had two melting peaks **[20]**, which were due to the melt - recrystallize - melt process of PLA. The pure PLA at melting temperature had only one peak, but in soda lignin /PLA, except for the 10% composite material, the other composite materials exhibited two melting peaks. This observation may be explained by a change in the crystallization behavior of the PLA matrix in the presence of lignin, with the region showing imperfect crystallization melting at a lower temperature.. The melting temperature with a perfect crystallization degree is lower, showing that the composite material had two melting absorption peaks **[21]**. In addition, with the increase of soda lignin content, the intensity of the melting peak in **Fig. 2** gradually increased, indicating that the amount of imperfect crystallization gradually increased. For 10 wt of soda lignin, the *Tg* of the composite increased to 61.8°C, indicating that the temperature of the softness and rubber properties of the composite increased to a certain extent. The cold crystallization temperature (Tcc) was shifted from 119.4°C to 114.4°C, indicating that soda lignin could promote the cold crystallization of PLA **[32]**. When lignin content was ≥ 20 wt%, Tg and Tcc of

the composite gradually shifted to low temperature with the increase of lignin content, because the molecular mobility of PLA matrix was changed by adding soda lignin.

Interestingly, an increase in PLA crystallinity with increasing soda lignin content has been observed: crystallinity rose gradually from 6.40 % to 9.07 % and then to 13.34 % for lignin contents of 0 % (PLA), 10% (PLA-L10) and 20 % (PLA-L20) respectively. Based on literature data, this can be explained by a nucleating effect of lignin on PLA**[33]**. However, when the lignin content reached 30%, the crystallinity of the composite (PLA-L30) dropped to 7.79%, due to the complex and irregular structure of the lignin. The presence of rigid units in the main chain and its cross-linked structure limit the movement of PLA chains. **[20]**. In addition, a high concentration of lignin favors its agglomeration, leading to biphasic separation with PLA and affecting its ability to crystallize.

The Tg of PEG-modified lignin/PLA composites was slightly higher than that of pure PLA, indicating that the upper limit for the service temperature of PEG-modified lignin/PLA was slightly increased, expanding its fields of application. From **Fig. 2** and **Table 5**, compared with the unmodified PLA composites, the melting temperature (Tm) of PEG-modified lignin/PLA composites had only one peak, indicating that the melting temperature with complete crystallization was not shifted. On the other hand, the Xc of PEG-modified lignin/PLA was reduced, probably because of the branched chain of PEG-modified lignin and the rigid crosslinking structures which restricted the movement of PLA chains **[22]**, affecting the crystallization ability and crystallization rate of the composites. Mw, Mn and Mw/Mn of PEG modified lignin

(**Table 4**) were larger than those of soda lignin, confirming grafting of PEG units and Tcc also increased (**Table 5**), probably because of the long chain of PEG which made the cold crystallization of the composite more difficult **[22]**. The Tm of modified lignin/PLA composites was maintained at around 154 °C, and the increase over pure PLA (153 °C) was negligible, demonstrating that the addition of modified lignin does not degrade the composites' heat resistance.

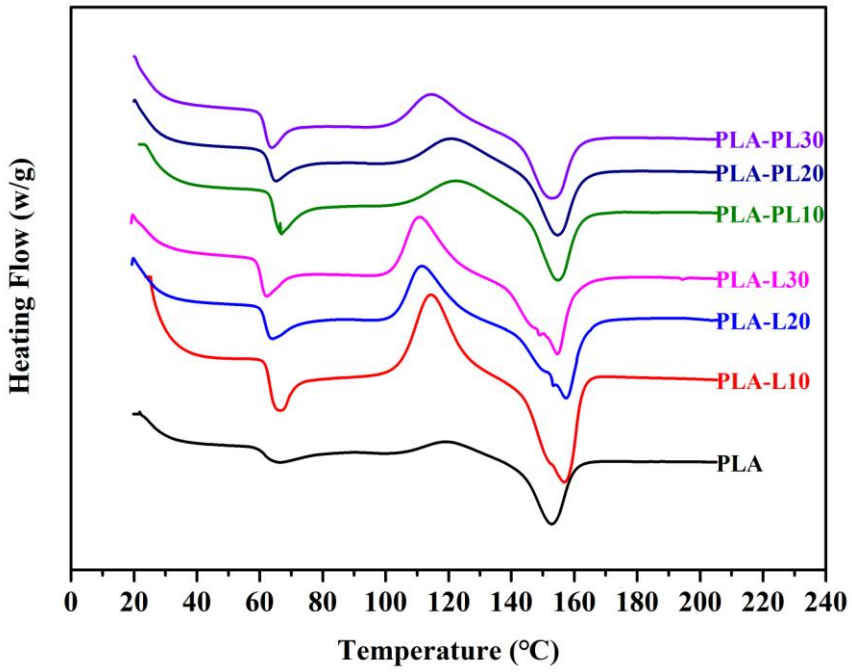

Figure 2 DSC thermograms of PLA and PLA/lignin composites

Table 5 Transition temperatures and enthalpies of PLA and PLA/lignin composites

Sample	Tg (°C)	Tcc (°C)	Hcc (J/g)	Tm (°C)	Hm (J/g)	X*c* (%)
PLA	59.3	119.4	9.4	153.0	15.4	6.40
PLA-L10	61.8	114.4	27.3	156.9	35.8	9.07
PLA-L20	60.4	111.7	17.4	157.6	29.9	13.34
PLA-L30	59.2	110.9	19.9	154.7	27.2	7.79
PLA-PL10	65.8	122.7	11.2	155.0	17.9	7.15
PLA-PL20	61.6	120.8	14.1	154.5	18.9	5.12
PLA-PL30	60.4	114.8	17.9	153.1	20.6	2.88

3.3 TGA

Fig. 3 showed the thermogravimetric (TG) and derivative thermogravimetric (DTG) of pure PLA and PLA/lignin composites. It can be seen from the **Fig. 3** that the degradation starting temperature (T_{dst}) of pure PLA was 295.5 °C, the maximum weight loss temperature (T_{dmax}) was 357.9 °C, and PLA had been almost completely thermally degraded at 381 °C. The thermal stability of lignin/PLA composites can be divided into three degradation stages **[20]**, the first is to evaporate water before 150 °C, the second is mainly the degradation of PLA between 150 - 400 °C, and the third is the gradual degradation of lignin after higher than 400 °C. As the lignin content increased, the T_{dst} and weight loss rate of composites decreased, the T_{dmax} fluctuated, and the residue rate increased. This indicated an improvement of flame retardancy of the material, because the residue produced by the thermal degradation of lignin can effectively prevent the contact of oxygen with the combustion area

(mainly PLA), thereby playing a flame retardant effect **[34]**. The specific thermogravimetric analysis data were shown in **Table 6**.

Compared with unmodified lignin, the T_{dst} and T_{dmax} of PEG modified lignin/PLA composites were increased. An increase in T_{dst} of PLA-PL10 compared to PLA-L10 from 233.1°C to 299.1°C was observed. This may be explained by lignin recondensation during the Pegylation reaction of lignin, induced by the acidic conditions used, producing thermally stable crossed linked lignin substructure. Compared with the pyrolysis process of pure PLA and unmodified lignin/PLA, the pyrolysis speed after modification was faster, mainly because PEG branched chain began to form chain-initiating groups under the effect of thermal activation, which provided a basis for subsequent chain breaking reactions **[22]**. After reaching a certain temperature, the chemical bonds of the molecular chain began to break on a large scale, which also led to a decrease in residues. These results therefore show an increase in the thermal stability of PEG-modified lignin/PLA.

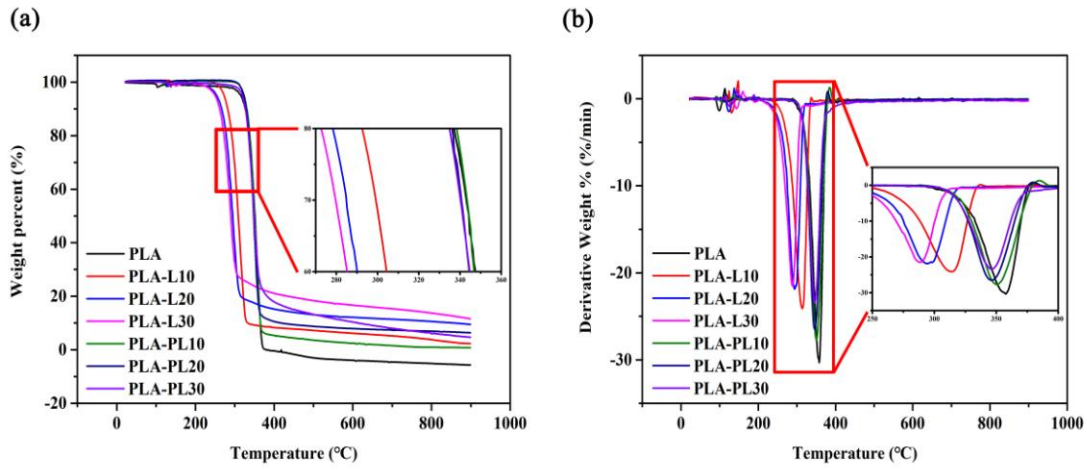

Figure 3 (a) TG and (b) DTG curves of different samples

Table 6 Thermal properties of different samples

Sample	PLA	PLA-L10	PLA-L20	PLA-L30	PLA-PL10	PLA-PL20	PLA-PL30
T_{dst}/°C	295.5	233.1	215.7	210.1	299.1	295.4	296.7
T_{dmax}/°C	357.9	313.8	294.3	288.4	350.5	346.2	347.1
Residue /%	--	2.49	9.61	11.61	0.77	6.51	4.82

3.4 DMA

DMA has been widely used to characterize the thermomechanical properties of composites to understand the viscoelastic behavior of matrix. **Fig. 4** showed the storage modulus (E′), loss modulus (E″), and loss factor (tanδ) of composites from room temperature to 80°C. From **Fig. 4a**, the E' of all samples shows a significant decrease with increasing temperature. According to the tanδ in **Fig. 4b**, the Tg of the PLA matrix was about 55 °C. PLA deformation is mainly caused by changes in bond length and angle. When the temperature reached Tg, the segment movement of PLA caused a peak in tanδ and displayed the characteristics of rubber. From **Fig. 4a**, it can be seen that the initial position E′ value of the composite was higher than that of pure PLA, indicating that the stiffness of PLA was increased by the addition of soda lignin and PEG modified lignin **[31]**. For soda lignin/PLA, Tg decreased with the addition of soda lignin, probably due to the low li gnin/matrix compatibility. With the addition of

PEG-modified lignin, E′ decreased compared with soda lignin/PLA composites at the same content, indicating that PEG-modified lignin had some plasticizing effect and improved the chains flexibility **[22]**. With increasing PEG-modified lignin content, E′ first increased until reaching a maximum for PLA-PL20. For PA-PL30 agglomeration phenomena leading to biphasic separation can be proposed **[22].** These results are similar to those of ATG.

The Tan δ was the loss factor, expressed as the ratio of the loss modulus to the storage modulus. As can be seen in **Fig. 4b**, the tan δ value gradually increased as the temperature raised until it reached Tg, and then gradually decreased. In accordance with DSC results, Tg shifted to low temperature with the increase of soda lignin content, which indicated that the increase of content affected the free movement ability of the molecular segment of PLA **[35]**. Tg of PEG-modified lignin/PLA were higher than those of pure PLA, indicating that the addition of modified lignin was beneficial in promoting the free movement of PLA segments. Tanδ value increased, possibly due to the presence of voids.

The loss modulus (E″) was the ability of a material to dissipate applied energy. E″ was sensitive to different molecular movements, transitions, morphological and structural heterogeneity. The curves of PLA and PLA composites were shown in **Fig. 4c**. At room temperature, pure PLA was found to have a lower E″ than composites **[35]**, the addition of lignin and PEG-modified lignin leading to an increase in molecular friction.

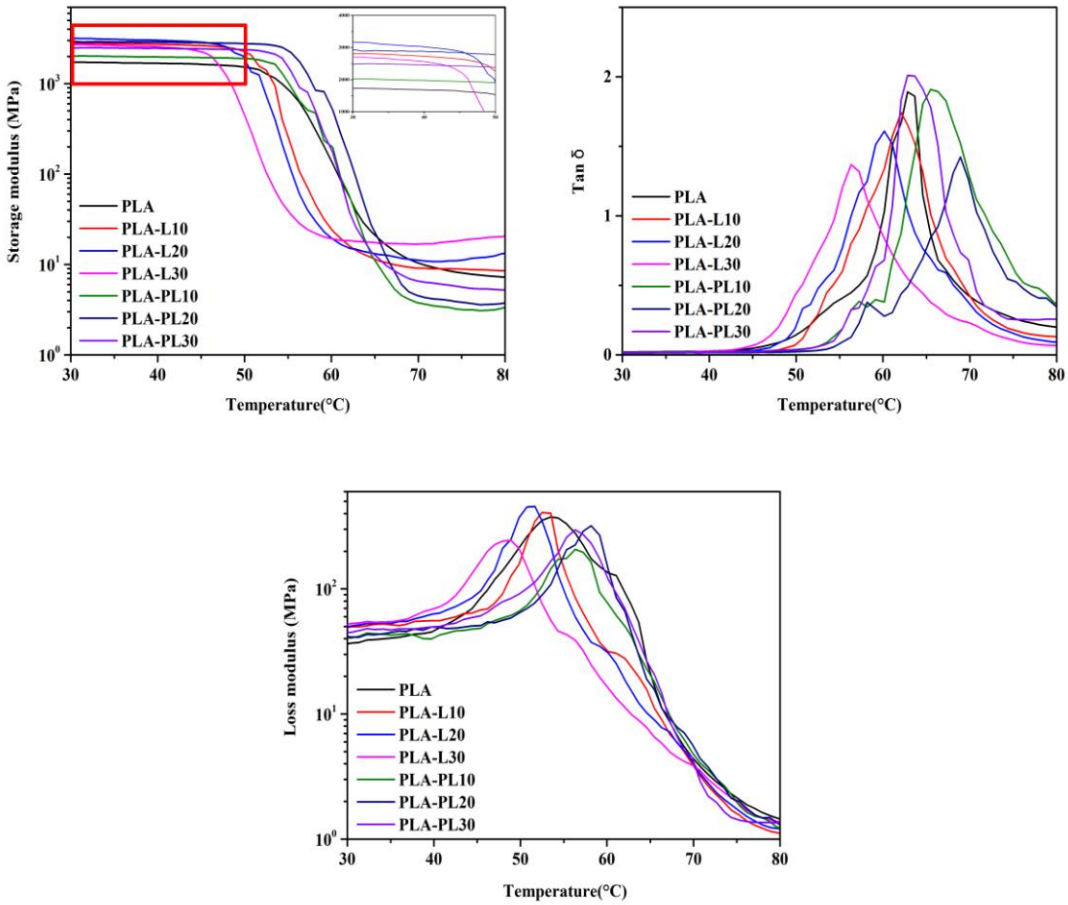

Figure 4 (a) Storage modulus, (b) Loss factor, and (c) Loss modulus of PLA and PLA / lignin composites

3.5 Mechanical testing

As a degradable polymer material, PLA has high strength and modulus, but the high price of PLA limits its wide application in agriculture and industry. The preparation of composite materials by adding cheap lignin to polylactic acid is an effective way to reduce the price of PLA products. **Fig. 5** showed the mechanical properties the lignin-based composites. The tensile strength and elongation at break were 67.51 MPa and 6.91% respectively for pure PLA , 51. 23 MPa and 3.71% for PLA-L10 and 45.71 MPa and 2.72% for PLA-L20, 40.67MPa, and 1.94%. for

PLA-L30. These results clearly indicated that the addition of lignin reduced the tensile strength and elongation at break of the material. In accordance with literature, this can be explained by the presence of lignin particles, which disrupt the formation of long-range continuous phase of PLA molecule **[22]**. As can be seen from SEM **Fig. 6**, the larger the size of the filler, the smaller the specific surface area, resulting in a smaller interface area and stress transfer between the matrix and the filler. In addition, the hydrogen bonding and polar interactions between soda lignin agglomeration and PLA matrix may also affect stress transfer between the matrix and filler. This was consistent with literature reports **[36]**. At the same time, the addition of soda lignin increased the tensile modulus of the composite to a certain extent. The tensile modulus reached 3.74 GPa for PLA-PL10 and 4.15 GPa for PLA-PL30, respectively 5.71% and 18.6% higher than that of pure PLA indicating that the addition of soda lignin can improve the overall stiffness and modulus of the composite **[36]**.

Interestingly, the tensile strength of PLA-PL10 compared to PLA-L10 increased from 51. 23 MPa to 62.55 MPa, an improvement of almost 22%. This confirmed the plasticizing effect of PEG-modified lignin. Combined with **Fig. 6**, it can be found that the modified lignin was better dispersed in PLA the particle size being smaller, resulting in a larger specific surface area, which increased the interfacial force between the matrix and the filler. At the same time, the intermolecular interactions between PEG branched chain and PLA further increased the strength of the composite. For the highest modified lignin content (PLA-PL30) and in line with the previous results, the decrease of tensile strength (51.41 MPa) observed is justified by

agglomeration phenomenon **[22, 37]**. The modulus of elasticity of PEG-modified lignin/PLA composites was smaller than that of unmodified composites because of the presence of the plasticity of PEG branched chains. All these results show that PLA-PL10 has excellent overall mechanical properties, preserving the tensile strength and elongation at break of pure PLA while increasing the material's modulus of elasticity.

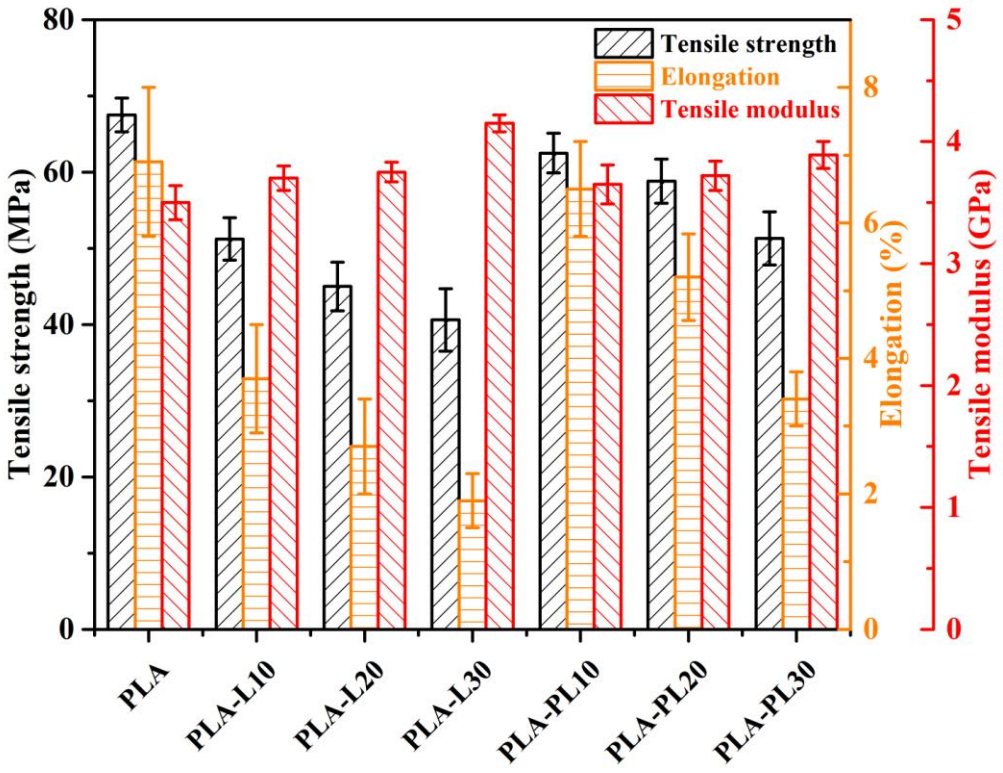

Figure 5 Mechanical properties of PLA, PLA-lignin and PLA-ligninplasticizer composites

3.6 Scanning Electron Microscopy

The surface and tear fractured surface of pure PLA and composites were observed, as shown in **Fig. 5** and **Fig. 6**. From the **Fig. 5**, even if the content of lignin

or PEG modified lignin was up to 30%, lignin can be uniformly dispersed in the PLA matrix. With the increase of lignin content, the particle size of lignin gradually increased. PEG-modified lignin had a smaller particle size than soda lignin at the same content. When the content of PEG-modified lignin reached 30% (**Fig. 6h**), cavities on the surface of the composite were observed due to agglomeration **[22]**.

The SEM for the tear fractured surface of the composite was shown in **Fig. 7**. PLA-L10 (**Fig. 7b2**) had a certain toughness indicating that the material section has a small amount of tensile wire drawing and has good tensile strength **[33, 38]**. For PLA-L20 and PLA-L30 (**Fig. 7d2** & **Fig. 7f2**), a large number of continuous gaps between PLA and filler appeared in the tear fractured surface of the composite, indicating a lack of interfacial bonding and a poor compatibility.

At the fractured surface of PLA/PEG-modified lignin composites, except where the lignin was pulled off as shown by arrows in **Fig. 7c2**, **7e2** and **7g2**, a very good PEG-modified lignin dispersion was observed and it was even almost impossible to distinguish the PLA matrix phase from the filler. This observation confirmed the above speculations regarding the strong force between the PLA and the PEG modified lignin and justified the improvement of tensile strength previously reported **[22, 38]**.

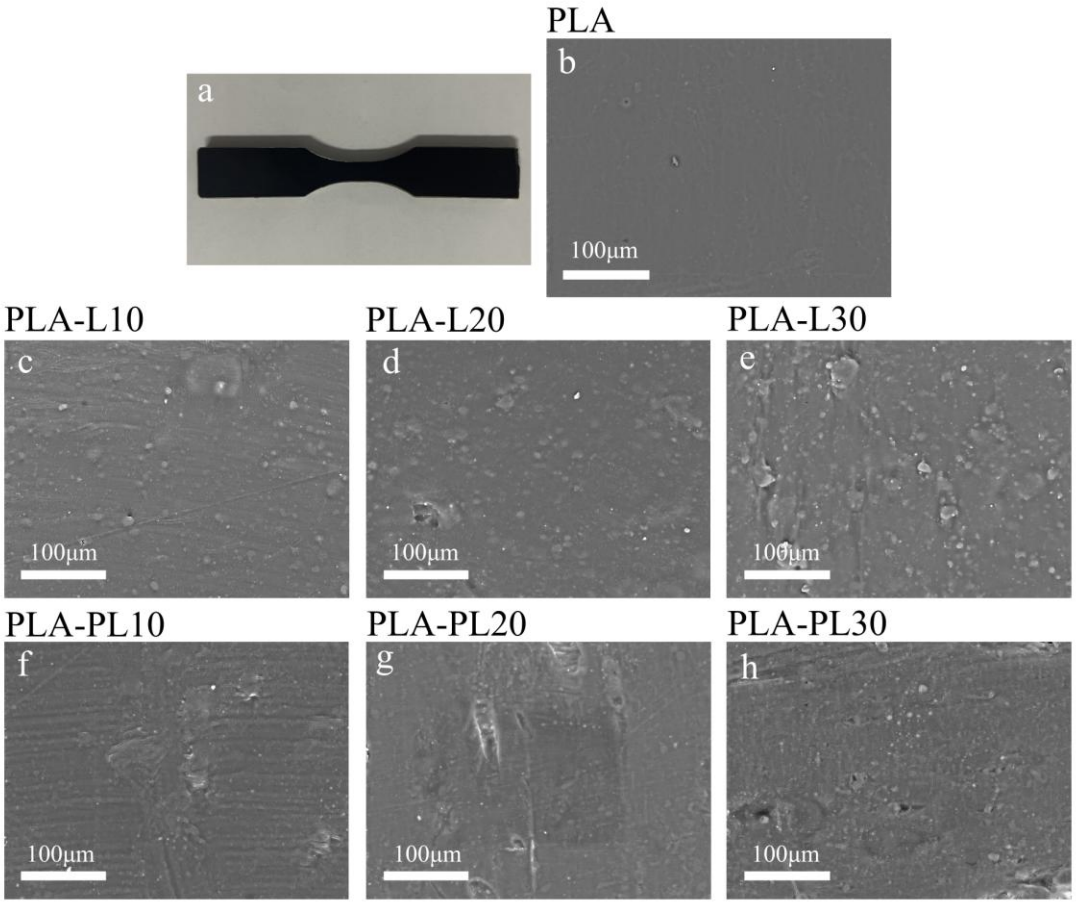

Figure 6 a) 3D printed dog bone sample, SEM images of surface (b, c, d, e f, g, h)

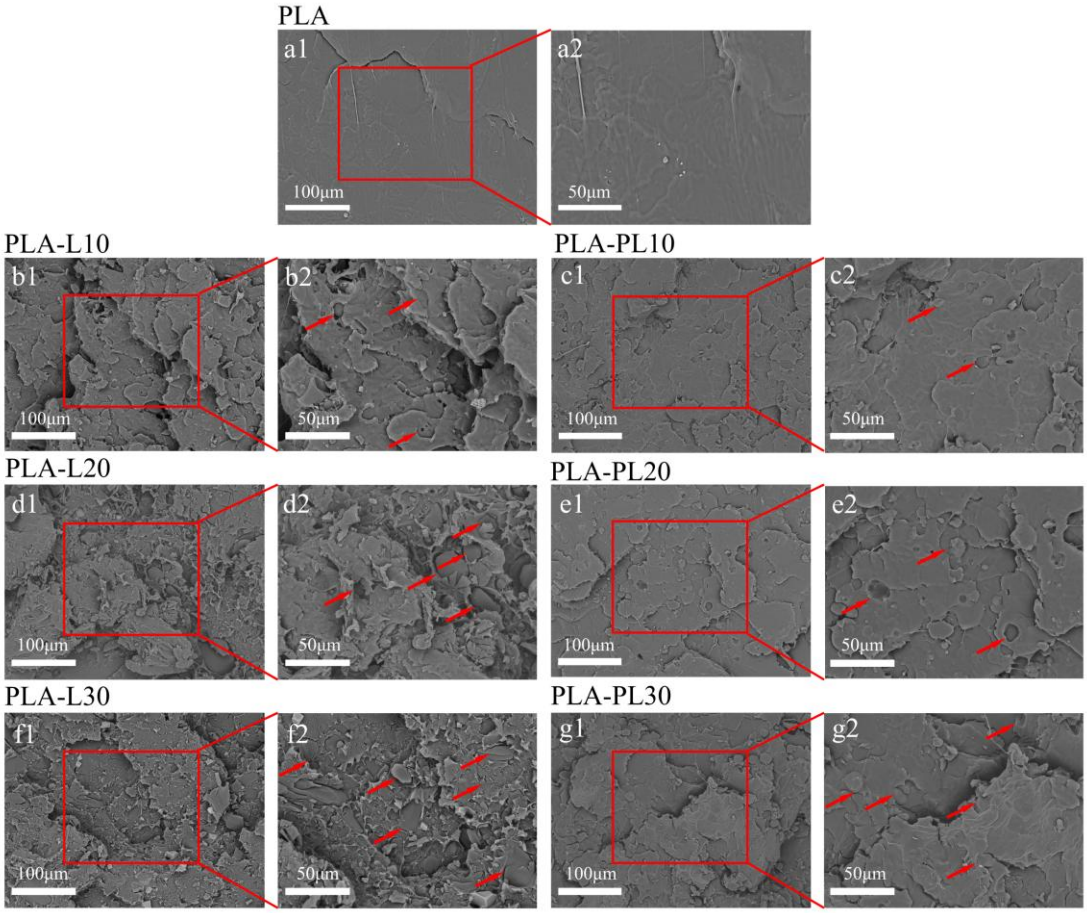

Figure 7 SEM images of a) PLA, b) PLA-L10, c) PLA-PL10, d) PLA-L20, e) PLA-PL20, f) PLA-L30, g) PLA-PL30 (red arrows indicate lignin aggregates)

3.7 Water absorption and degradation in solvent

Fig. 8a gives the water absorption of lignin/PLA composites with different lignin contents by immersing in deionized water **[39]**. As can be seen from **Fig. 8a**, PLA/lignin composites displayed higher water absorption than pure PLA and the water absorption rate increased with the lignin content. This is due to the hydrophilic nature of lignin and the presence of OH units promoting intermolecular hydrogen bonds with water molecules **[40, 41]**. In addition, the presence of pores at the interface PLA/filler described above for composites with high lignin contents (**Fig. 6**

and **Fig. 7**) promotes water penetration after full immersion. On the other hand, PEG-modified lignin/PLA composites had lower water absorption than unmodified composites, mainly because a better interface between modified lignin and PLA matrix **[22]**. **Fig. 8b** was the residual amounts of lignin/PLA with different lignin content composites immersed in three buffer solutions. All samples exhibited higher degradation rates than pure PLA in the three buffer solutions. The greater the amount of lignin, the better composite's degradation performance. As seen in Fig 8b, degradation depends on the pH of the medium: increasing pH favors degradation . At the same content, PEG-modified lignin/PLA composites showed a lower degradation rate than soda lignin/PLA composites **[42]**, which was mainly due to the good compatibility between tPEG-modified lignin and PLA.

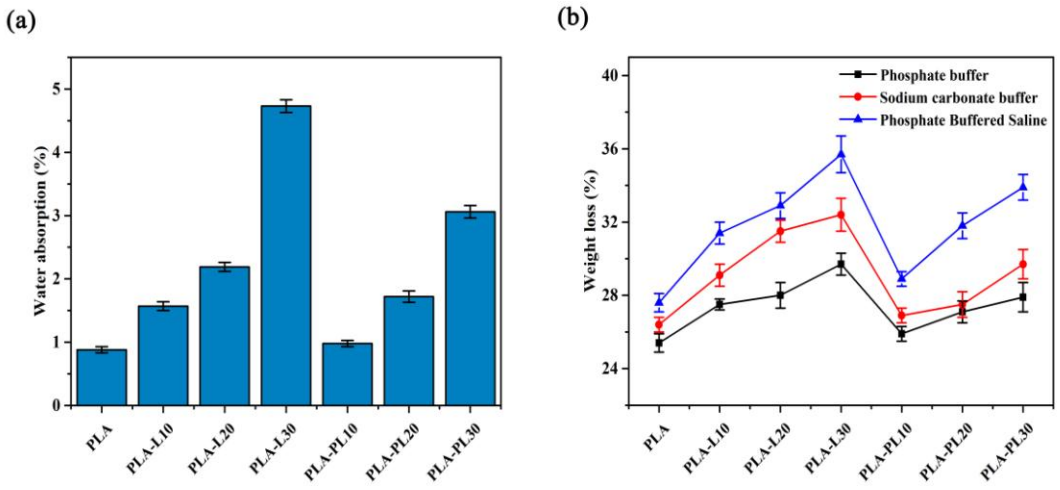

Figure 8 Water absorption of PLA with various lignin contents over 50 days(a) and degradation in different solvent media over 50 days (b)

Conclusion

In this paper, the comprehensive properties of PEG-modified lignin in PLA composites were studied. PEG-modified lignin displayed a good dispersion and compatibility with PLA and increased its melting and glass transition temperatures, The composite material produced by the mixing of PEG modified lignin and PLA can not only reduce the cost of high production cost, improve poor heat resistance, maintain tensile properties, but also make up for the shortcomings of a single material, achieve complementary advantages, and have good practical value.

CRediT authorship contribution statement

Zehui Ju: Investigation, Conceptualization, Formal analysis, Writing - original draft. **Nicolas Brosse**: Conceptualization, Methodology, Writing - review & editing. **Sandrine Hoppe**: Writing - review & editing. **Zhiqiang Wang**: Sample preparation, Structure fabrication. **Isabelle Ziegler-Devin**: Data curation. **Haiyang Zhang**: Formal analysis. All authors read and contributed to the manuscript.

Declaration of Competing Interest

The authors declare that they have no known competing financial interests or personal relationships that could have appeared to influence the work reported in this paper.

Acknowledgements

The authors gratefully acknowledge funding supports from the Start-up Funds

for Scientific Research at the Nanjing Forestry University (No. 163020342), the National Key Research and Development Program of China (2021YFD2200605) and Qing Lan Project of Zhiqiang Wang. LERMAB is supported by the French National Research Agency through the Laboratory of Excellence ARBRE (ANR-12-LABXARBRE-01).

Reference

[1] T.R. Swetha, V. Ananthi, A. Bora, N. Sengottuvelan, K. Ponnuchamy, G. Muthusamy, A. Arun, A review on biodegradable polylactic acid (PLA) production from fermentative food waste - Its applications and degradation. Int. J. Biol. Macromol. 234 (2023) 123703, https://doi.org/10.1016/j.ijbiomac.2023.123703.

[2] J.-Y. Lee, J. An, C.K. Chua, Fundamentals and applications of 3D printing for novel materials. Appl. Mater. Today 7 (2017) 120-133. https://doi.org/10.1016/j.apmt.2017.02.004.

[3] S.Wasti, S. Adhikari, Use of biomaterials for 3D printing by fused deposition modeling technique: a review. Front. Chem. 8 (2020) 1-14. https://doi.org/10.3389/ fchem.2020.00315.

[4] H. Kyutoku, N. Maeda, H. Sakamoto, H. Nishimura, K. Yamada, Effect of surface treatment of cellulose fiber (CF) on durability of PLA/CF bio-composites. Carbohydr. Polym. 203 (2019) 95-102. doi: 10.1016/j.carbpol.2018.09.033.

[5] J. Ren, Biodegradable poly (lactic acid) synthesis, modification, processing and applications. Tsinghua University Press : Springer, Beijing; Heidelberg. (2011).

[6] K.J. Jem, B. Tan, The development and challenges of poly (lactic acid) and poly (glycolic acid). Advanced Industrial and Engineering Polymer Research. 3 (2020) 60-70. https://doi.org/10.1016/j.aiepr.2020.01.002.

[7] M.A. Cuiffo, J. Snyder, A.M. Elliott, N. Romero, S. Kannan, G.P. Halada, Impact of the fused deposition (FDM) printing process on polylactic acid (PLA)

chemistry and structure. Appl. Sci. 7 (2017) 579. https://doi.org/10.3390/app7060579.

[8] O. Gordobil, I. Egü´es, R. Llano-Ponte, J. Labidi, Physicochemical properties of PLA lignin blends. Polym. Degrad. Stabil. 108 (2014) 330-8. https://doi.org/10.1016/j. polymdegradstab.2014.01.002.

[9] P.K. Bajpai, I. Singh, J. Madaan, Development and characterization of PLA-based green composites: a review. J. Thermoplast. Compos. Mater. 27 (2014) 52-81. https://doi.org/10.1177/0892705712439571.

[10] A. Basu, M. Nazarkovsky, R. Ghadi, W. Khan, A.J. Domb, Poly(lactic acid)- based nanocomposites. Polym. Adv. Technol. 28 (2017) 919-930. https://doi.org/10.1002/pat.3985.

[11] E. Gkartzou, E.P. Koumoulos, C.A. Charitidis, Production and 3D printing processing of bio-based thermoplastic filament. Manuf. Rev. 4 (2017) 1. https://doi.org/ 10.1051/mfreview/2016020.

[12] W. Xu, A. Pranovich, P. Uppstu, X. Wang, D. Kronlund, J. Hemming, H. Öblom, N. Moritz, M. Preis, N. Sandler, S. Willför, C. Xu, Novel biorenewable composite of wood polysaccharide and polylactic acid for three dimensional printing. Carbohydr. Polym. 187 (2018) 51-8. https://doi.org/10.1016/ j.carbpol.2018.01.069.

[13] J. Lisperguer, P. Perez, S. Urizar, Structure and thermal properties of lignins: characterization by infrared spectroscopy and differential scanning calorimetry. J. Chil. Chem. Soc. 54 (2009) 460-463. http://dx.doi.org/10.4067/S0717-97072009000400030.

[14] S.-Y. Jeong, E.-J. Lee, S.-E. Ban, J.-W. Lee, Structural characterization of the lignin-carbohydrate complex in biomass pretreated with Fenton oxidation and hydrothermal treatment and consequences on enzymatic hydrolysis efficiency. Carbohydr. Polym. 279 (2012) 118375. https://doi.org/10.1016/j.carbpol.2021.118375.

[15] D.-S. Bajwa, G. Pourhashem, A.-H. Ullah, S.-G. Bajwa, A concise review of current lignin production, applications, products and their environmental impact.

Ind. Crop. Prod. 139 (2019) 111526. https://doi.org/10.1016/j.indcrop.2019.111526.

[16] A.K. Mondal, M.T. Uddin, S.M.A. Sujan, Z. Tang, D. Alemu, H.A. Begum, J. Li, F. Huang, Y. Ni, Preparation of lignin-based hydrogels, their properties and applications. Int. J. Biol. Macromol. 245 (2023) 125580. https://doi.org/10.1016/j.ijbiomac.2023.125580.

[17] L. Xu, S.J. Zhang, C. Zhong, B.Z. Li, Y.J. Yuan, Alkali-Based Pretreatment-Facilitated Lignin Valorization: A Review. Industrial & Engineering Chemistry Research, 59 (2020) 16923-16938. https://doi.org/10.1021/acs.iecr.0c01456.

[18] D. Kai, M.J. Tan, P.L. Chee, Y.K. Chua, Y.L. Yap, X.J. Loh, Towards lignin-based functional materials in a sustainable world. Green Chem. 18 (2016) 1175-1200. https://doi.org/10.1039/C5GC02616D.

[19] Y. Wang, J. Hou, Y. Huang, Y. Fu, Structure-controlled lignin complex for PLA composites with outstanding antibacterial, fluorescent and photothermal conversion properties. Int. J. Biol. Macromol. 194 (2022) 1002-1009. https://doi.org/10.1016/j.ijbiomac.2021.11.159.

[20] H. Ye, Y. He, H. Li, T. You, F. Xu, 3D-Printed Polylactic Acid/Lignin Films with Great Mechanical Properties and Tunable Functionalities towards Superior UV-Shielding, Haze, and Antioxidant Properties. Polymers. 15 (2023) 2806. https://doi.org/10.3390/polym15132806.

[21] M. Tanase-Opedal. E. Espinosa, A. Rodríguez, G. Chinga-Carrasco, Lignin: a biopolymer from forestry biomass for biocomposites and 3D printing. Materials. 12 (2019) 1-15. https://doi.org/10.3390/ma12183006.

[22] S. Wasti, E. Triggs, R. Farag, M.L. Auad, S. Adhikari, D.S. Bajwa, M. Li, A.J. Ragauskas, Influence of plasticizers on thermal and mechanical properties of biocomposite filaments made from lignin and polylactic acid for 3D printing. Compos. B Eng. 205, (2021) 108483. https://doi.org/10.1016/j.compositesb.2020.108483.

[23] J. Guo, X. Chen, J. Wang, Y. He, H. Xie, Q. Zheng, The Influence of

Compatibility on the Structure and Properties of PLA/Lignin Biocomposites by Chemical Modification. Polymers. 12 (2020) 56. https://doi.org/10.3390/polym12010056.

[24] Y. Kim, J. Suhr, H.W. Seo, H. Sun, S. Kim. I.K. Park, S.H. Kim, Y. Lee, K.J. Kim, J.D. Nam, All Biomass and UV Protective Composite Composed of Compatibilized Lignin and Poly (Lactic-acid). Sci Rep. 7 (2017) 43596. https://doi.org/10.1038/srep43596.

[25] M. Li, C.G. Yoo, Y. Pu, A.K. Biswal, A.K. Tolbert, D. Mohnen, A.J. Ragauskas, Downregulation of pectin biosynthesis gene GAUT4 leads to reduced ferulate and lignin-carbohydrate cross-linking in switchgrass. Commun. Biol. 2 (2019) 1-11. https://doi.org/10.1038/s42003-018-0265-6.

[26] Q. He, I. Ziegler-Devin, L. Chrusciel, S.N. Obame, L. Hong, X. Lu, N. Brosse, Lignin-First Integrated Steam Explosion Process for Green Wood Adhesive Application. ACS Sustain. Chem. Eng. 8 (2020) 5380-5392. https://doi.org/10.1021/acssuschemeng.0c01065.

[27] S. Nakagame, R.-P. Chandra, J.-F. Kadla, J.-N. Saddler, The isolation, characterization and effect of lignin isolated from steam pretreated Douglas-fir on the enzymatic hydrolysis of cellulose. Bioresource Technol. 102 (2011) 4507-4517. https://doi.org/10.1016/j.biortech.2010.12.082.

[28] Y. Feng, J. Lan, P. Ma, X. Dong, J. Qu, H. He, Chemical structure and thermal properties of lignin modified with polyethylene glycol during steam explosion. Wood. Sci. Technol. 51 (2017) 135-150. https://doi.org/10.1007/s00226-016-0870-9.

[29] T.-T. Nge, Y. Tobimatsu, S. Takahashi, E. Takata, M. Yamamura, Y. Miyagawa, T. Ikeda, T. Umezawa, T. Yamada, Isolation and Characterization of Polyethylene Glycol (PEG)-modified Glycol Lignin via PEG Solvolysis of Softwood Biomass in a Large-scale Batch Reactor. ACS Sustain. Chem. Eng. 6 (2018) 7841-7848. https://doi.org/10.1021/acssuschemeng.8b00965.

[30] S.-N. Obame, I. Ziegler-Devin, R. Safou-Tchima, N. Brosse, Homolytic and heterolytic cleavage of beta-ether linkages in hardwood lignin by Steam

Explosion. J. Agr. Food. Chem. 67 (2019) 5989-5996. https://doi.org/10.1021/acs.jafc.9b01744.

[31] J.H. Choi, J.H. Kim, S.Y. Lee, S.K. Jang, H.W. Kwak, H. Kim, I.G. Choi, Thermoplasticity reinforcement of ethanol organosolv lignin to improve compatibility in PLA-based ligno-bioplastics: Focusing on the structural characteristics of lignin. Int J Biol Macromol. 209 (2022) 1638-1647. https://doi.org/10.1016/j.ijbiomac.2022.04.090.

[32] M.A.S. Anwer, H.E. Naguib, A. Celzard, V. Fierro, Comparison of the thermal, dynamic mechanical and morphological properties of PLA-Lignin & PLA-Tannin particulate green composites. Compos. B Eng. 82 (2015) 92-9. https://doi.org/10.1016/j. compositesb.2015.08.028.

[33] J. Liao, N. Brosse, A. Pizzi, S. Hoppe, X. Zhou, G. Du, Characterization and 3D printability of poly (lactic acid)/acetylated tannin composites. Industrial Crops and Products, 149 (2020) 112320. https://doi.org/10.1016/j.indcrop.2020.112320.

[34] M. Boruvka, L. Behalek, P. Lenfeld, C. Ngaowthong, M. Pechociakova, Structurerelated properties of bionanocomposites based on poly(lactic acid), cellulose nanocrystals and organic impact modifier. Mater. Technol. 34 (2019) 143-156. https://doi.org/10.1080/10667857.2018.1540332.

[35] M. Idrees, S. Jeelani, V. Rangari, Three-dimensional-printed sustainable biocharrecycled PET composites. ACS Sustainable. Chem. Eng. 6. (2018) 13940-8. https://doi.org/ 10.1021/acssuschemeng.8b02283.

[36] S.-Y. Fu, X.-Q. Feng, B. Lauke, Y.-W. Mai, Effects of particle size, particle/matrix interface adhesion and particle loading on mechanical properties of particulate-polymer composites. Compos. Part B Eng. 39 (2008) 933-961. https://doi.org/10.1016/j.compositesb.2008.01.002.

[37] B.W. Chieng, N.A. Ibrahim, WMZW. Yunus, M.Z. Hussein, Plasticized poly(lactic acid) with low molecular weight poly(ethylene glycol): mechanical, thermal, and morphology properties. J. Appl. Polym. Sci. 130 (2013) 4576-80. https://doi.org/ 10.1002/app.39742.

[38] K. Sungsanit, N. Kao, S.N. Bhattacharya, Properties of linear poly (lactic acid)/

polyethylene glycol blends. Polym. Eng. Sci. (2012) 108–16. https://doi.org/10.1002/ pen.

[39] L. Zhang, S. Lv, C. Sun, L. Wan, H. Tan, Y. Zhang, Effect of MAH-g-PLA on the properties of wood Fiber/Polylactic acid composites. Polymers 9 (2017) 591. https://doi.org/10.3390/polym9110591.

[40] O. Gordobil, I. Egü´es, J. Labidi, Modification of Eucalyptus and Spruce organosolv lignins with fatty acids to use as filler in PLA. React. Funct. Polym. 104 (2016) 45-52. https://doi.org/10.1016/j.reactfunctpolym.2016.05.002.

[41] G.H. Yew, A.M. Mohd Yusof, Z.A. Mohd Ishak, U.S. Ishiaku, Water absorption and enzymatic degradation of poly(lactic acid)/rice starch composites. Polym. Degrad. Stab. 90 (2005) 488-500. https://doi.org/10.1016/j.polymdegradstab.2005.04.

[42] M.A. Elsawy, K.-H. Kim, J.-W. Park, A. Deep, Hydrolytic degradation of polylactic acid (PLA) and its composites. Renewable Sustainable Energy Rev. 79 (2017) 1346-1352. https://doi.org/10.1016/j.rser.2017.05.143.